

Cite this: *Chem. Commun.*, 2012, **48**, 1027–1029

www.rsc.org/chemcomm

# Catalyst-free synthesis of iodine-doped graphene *via* a facile thermal annealing process and its use for electrocatalytic oxygen reduction in an alkaline medium†

Zhen Yao, Huagui Nie, Zhi Yang,\* Xuemei Zhou, Zheng Liu and Shaoming Huang\*

Received 5th October 2011, Accepted 23rd November 2011

DOI: 10.1039/c2cc16192c

**Iodine-doped graphene has been successfully fabricated through a simple, economical, and scalable approach. The new metal-free catalyst can exhibit a high catalytic activity, long-term stability, and an excellent methanol tolerance for the oxygen reduction reaction.**

A fuel cell is a clean, high-efficient energy conversion device that converts the chemical energy from a fuel into electricity through a chemical reaction with oxygen. However, oxygen reduction reactions (ORR) with a complex four-electron transfer process are sluggish in nature and traditionally require the exclusive use of platinum-based catalysts.<sup>1</sup> Because of the high cost, scarce supply and poor durability of Pt, substantial efforts have been dedicated to improving its performance and to the search for non-noble metal catalysts (NPMC).<sup>2</sup>

Recently, various metal-free, N-doped carbon materials,<sup>3</sup> including carbon nanotubes and ordered mesoporous graphitic arrays, have been proposed as potential candidates for replacing Pt-based catalysts for ORR because they not only exhibit excellent electrocatalytic activities but also are inexpensive, durable, and environmentally friendly. Very recently, other heteroatom-doped carbon materials (*e.g.*, P-doped graphite layer and B-doped CNTs) have also been shown to possess pronounced catalytic activity for ORR.<sup>4</sup> The interesting findings suggest the possibility of identifying other element-doped graphite materials with high electrocatalytic activities for ORR.

Graphene, the parent of all graphitic forms, has shown many intriguing properties, including superior electrical conductivity, a large surface area, and high chemical stability, and has aroused considerable interest in a wide range of fields.<sup>5</sup> Theoretical calculations have shown that the introduction of heteroatoms (*e.g.*, N, P and B) into sp<sup>2</sup>-hybridized carbon frameworks in graphene is very effective in improving electrochemical performance of carbon.<sup>6</sup> According to Hu's reports involving the origin of this ORR activity enhancement with the N (or B) doped carbon materials, breaking the electroneutrality of graphitic materials between carbon and the dopant would

create favorable positive charged sites for the side-on O<sub>2</sub> surface adsorption, and is very favorable for promoting ORR.<sup>4</sup> Iodine has been widely applied in conducting polymers as an important dopant that improves the electrical conductivity of materials.<sup>7</sup> Moreover, it has also been noted that graphene has a similar conjugate structure to conducting polymers. The recent research has confirmed that the charge transfer doping of iodine in few-layer graphene has been achieved as an intercalated layer with a post deposition process.<sup>8</sup> These above-mentioned factors motivated us to explore the use of graphenes doped with iodine as electrocatalysts for ORR. Recently, some investigations involving the preparation of iodine-doped carbon materials have been reported,<sup>8</sup> but the research into iodine-doped graphenes as ORR catalysts in FCs is rare.

Herein, we introduce a simple, economical, and scalable route for the fabrication of iodine-doped graphene (I-graphene). The structure of the I-graphene was characterized through X-ray photoelectron spectroscopy (XPS) and Raman spectroscopy. The electrocatalytic performances show that the I-graphene can exhibit better catalytic activity and long-term stability than a commercial Pt/C catalyst. Our work not only successfully creates a new type of NPMC with excellent electrocatalytic activity but also provides further insights into the ORR mechanism with metal-free doped carbon materials.

The experimental scheme for I-graphene preparation is illustrated in Fig. 1. Briefly, I-graphenes were prepared by annealing graphene oxide (GO) and iodine at 500–1100 °C in argon. The contents and bonding configurations of iodine in these I-graphenes can be adjusted by varying either the mass ratios of GO and iodine or the annealing temperature. As a

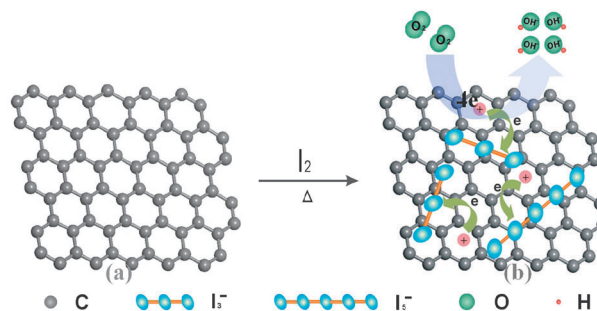
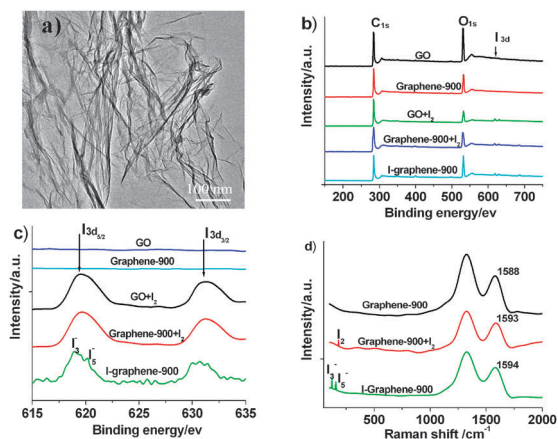


Fig. 1 Schematic illustration of I-graphene preparation.

Nanomaterials and Chemistry Key Laboratory,  
Wenzhou University Wenzhou, 325027, P. R. China.  
E-mail: yang201079@126.com, smhuang@wzu.edu.cn;  
Fax: +86 577-8837-3064

† Electronic supplementary information (ESI) available: Experimental section, XPS spectrum, physical parameters and electrochemical properties of these graphenes. See DOI: 10.1039/c2cc16192c



**Fig. 2** (a) TEM of I-graphene-900, (b) XPS survey spectra and (c) high-resolution  $I_{3d}$  spectra of GO, Graphene-900, GO +  $I_2$ , Graphene-900 +  $I_2$  and I-graphene-900, (d) Raman spectra of Graphene-900, Graphene-900 +  $I_2$  and I-graphene-900.

control experiment, GO without an iodine dopant was treated under the same conditions. The resulting materials are denoted graphene-500, I-graphene-500, graphene-700, I-graphene-700, graphene-900, I-graphene-900, graphene-1100, and I-graphene-1100. Their physical parameters, electrochemical properties, and corresponding experimental data are listed in Table S1 (ESI†).

Fig. 2a presents a typical TEM image of I-graphene-900. It can be seen from Fig. 2a that the material is transparent, with a wrinkled and voile-like feature. The XPS survey spectrum of I-graphene-900 in Fig. 2b reveals a predominant  $C_{1s}$  peak (284.5 eV), an  $O_{1s}$  peak (532.0 eV) and two  $I_{3d}$  peaks ( $\sim 619.5$  eV,  $\sim 631.9$  eV), which confirm the presence of elemental iodine in I-graphene-900. The iodine-bonding configurations can be seen from XPS high-resolution  $I_{3d}$  spectra as shown in Fig. 2c. Unlike the  $I_{3d}$   $5/2$  peaks for Graphene-900 +  $I_2$  (mixture of Graphene-900 and  $I_2$ ) and GO +  $I_2$  (mixture of GO and  $I_2$ ), the  $I_{3d}$   $5/2$  for I-graphene-900 appears as two split peaks, at 618.6 and 620.2 eV, which can be attributed to triiodide ( $I_3^-$ ) and penta-iodide ( $I_5^-$ ), respectively.<sup>7</sup> The Raman spectroscopy in Fig. 2d shows that the G peaks of I-graphene-900 samples up-shifted to  $1594\text{ cm}^{-1}$ , compared to the Graphene-900's peak at  $1588\text{ cm}^{-1}$ . This result is coincident with the previous report involving I-doped graphene and is an important characteristic of p-type surface transfer doping of graphene.<sup>6</sup> At lower wave numbers, two new Raman peaks at  $117\text{ cm}^{-1}$  and  $154\text{ cm}^{-1}$  can be observed for I-graphene-900 compared with Graphene-900, which should be assigned to  $I_3^-$  and  $I_5^-$ , respectively.<sup>7,8</sup> On the other hand, there is no Raman peak corresponding to molecular iodine ( $181\text{ cm}^{-1}$ ), which further negates the possibility of physical accumulation of molecular iodine on the doped graphene surface. The Raman and XPS results are very similar with Kalita's report involving I-doped graphene,<sup>8</sup> and confirmed that iodine doping of graphene can be achieved using our approach, and the electron transfer between atomic iodine and graphene surface induces the presence of polyiodides with negative charge ( $I_3^-$  and  $I_5^-$ ) and graphene with positive charge. Fig. 1b shows the structure scheme of the I-graphene. According to previous reports,<sup>4</sup> we speculate that the positive charge is very favorable for adsorbing  $O_2$  onto the surface of graphene and then promoting ORR.

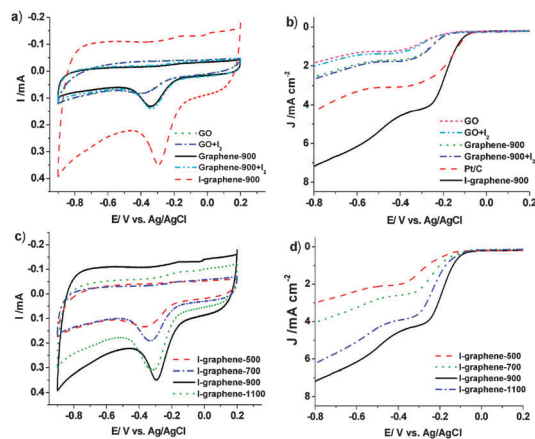


**Fig. 3** (a, c) Cyclic voltammograms for various graphenes, (b, d) LSV curves for various graphenes and a Pt/C catalyst on a glass carbon rotating disk electrode saturated in  $O_2$  at a scan rate of  $10\text{ mV s}^{-1}$  and a rotation rate of 1600 rpm.

The electrocatalytic activities of the graphene samples were evaluated using cyclic voltammetry (CV) measurements in 0.1 M KOH solution saturated with  $N_2$  or  $O_2$ . Fig. 3a clearly shows the ORR peaks for all of the samples (GO, GO +  $I_2$ , Graphene-900, Graphene-900 +  $I_2$  and I-graphene-900) in  $O_2$ -saturated conditions. For the GO electrode, a single cathodic reduction peak is present at  $-0.38\text{ V}$ . After the addition of pure iodine molecules, no noticeable change was observed in the ORR peak potential and current for the GO +  $I_2$  electrode, compared to the GO electrode. A similar phenomenon can also be observed for the Graphene-900 and Graphene-900 +  $I_2$  electrodes. Furthermore, from Fig. 3a, it can be also found that I-graphene-900 shows the highest peak current and the most positive ORR peak potential in all the graphene materials. The results suggest that the simple physical accumulation of molecular iodine on the doped graphene surface is not helpful for enhancing the ORR activity of graphene, while iodine surface transfer doping may be a very effective strategy.

To gain further insight into ORRs with these graphene samples, linear sweep voltammetry (LSV) measurements were performed on a rotating-disk electrode (RDE) in  $O_2$ -saturated 0.1 M KOH at a rotation rate of 1600 rpm. As a control, we also performed the LSV measurement for a commercial Pt/C electrocatalyst. As shown in Fig. 3b, it can be seen that the I-graphene-900 had the most positive onset potentials and highest current density amongst the graphene materials. This result is in agreement with the CV observations and further confirms that I doping can significantly enhance the ORR catalytic activity of graphene. Furthermore, from Fig. 3b, we can also observe that the onset potential for I-graphene-900 is close to that of the Pt/C catalyst and that its current density is higher than that of the Pt/C catalyst. These results suggest that the ORR catalytic activity of I-graphene-900 is better than that of commercial Pt/C catalysts. To further prove the role of I-graphene-900 throughout the ORR electrochemical process, we also performed RDE measurements at various rotating speeds. The limited diffusion current densities ( $J_L$ ) depend on the rotation rates, and the number of electron transfers ( $n$ ) involved in the ORR can be calculated from the Koutecky–Levich equation (see Fig. S1 and Table S1, ESI†).<sup>3</sup> The number of electron

transfers for I-graphene-900 was calculated to be 3.86 at  $-0.30$  V, which indicates a four-electron-transfer reaction. The calculated limited-kinetics current density ( $J_k$ ) value is  $9.21 \text{ mA cm}^{-2}$  at  $-0.30$  V. The electrocatalytic activity of I-graphene-900 is comparable to those of non-precious metal catalysts (e.g. N-doped CNTs,  $\text{Co}_3\text{O}_4/\text{N-graphene}$ ) in an alkaline electrolyte.<sup>2,3</sup> The above results further confirm that I-graphene-900 is a promising metal-free NPMC with high catalytic activity for ORR.

The stabilities and possible crossover effects of catalytic materials are also very important for practical applications. Therefore, the electrocatalytic selectivity of I-graphene-900 was measured *versus* the electro-oxidation of methanol. It can be seen from Fig. S2a (ESI<sup>†</sup>) that after the addition of 3 M methanol to a 0.1 M KOH solution saturated with  $\text{O}_2$ , no noticeable change was observed in the ORR current at the I-graphene-900 electrode. This indicates that the I-graphene-900 bears a high selectivity towards the ORR and has a good ability for avoiding crossover effects. The durabilities of the I-graphene-900 and Pt/C catalysts were compared. The catalysts were held at  $-0.30$  V for 18 000 s in an  $\text{O}_2$  saturated 0.1 M KOH solution, at an agitation rate of 1600 rpm. From Fig. S2b (ESI<sup>†</sup>), it can be seen that the I-graphene-900 exhibited a very slow decrease and a high relative current of 83.1% after 18 000 s. In contrast, the Pt/C electrode exhibits a gradual decrease, with a current loss of approximately 70.5% after 18 000 s. These results confirm that I-graphene-900 is highly promising for use in methanol and alkaline fuel cells.

As a control experiment, the influence of the annealing temperature on the electrocatalytic properties of the graphenes was further explored because the pyrolysis temperature can significantly affect the amounts of I elemental compositions and bonding configurations. Fig. 3c and d show the CV and LSV measurement curves for graphene samples obtained at 500–1100 °C. In addition, their physical parameters, corresponding experimental data, and electrochemical activity data are listed in Table S1 (ESI<sup>†</sup>). From Fig. 3c, it can be found that the doped graphene obtained at 900 °C (I-graphene-900) shows the highest peak current and most positive ORR peak potential of all the graphene samples. The results of LSV measurement shown in Fig. 3d also support the CV observations and all the observations strongly indicate that I-graphene-900 holds the most outstanding ORR activity amongst the graphene samples. To further elucidate the correlations among the structures, compositions, and catalytic activities of these I-graphenes obtained at different annealing temperatures, the high-resolution XPS (Fig. S3, ESI<sup>†</sup>) correlated with their corresponding electrochemical data were again analyzed. Remarkably, from Fig. S3 (ESI<sup>†</sup>), we find that the shape of the  $\text{I}_{3d}$  peaks significantly changes when the pyrolysis temperature is changed, thus suggesting that different amounts of I-bonding configurations are formed at different temperatures. In Table S1 (ESI<sup>†</sup>), it is noted that I-graphene-500 and I-graphene-700 had higher iodine content than that of I-graphene-900 but actually exhibited lower selectivity and catalytic activity. This indicates that the iodine content is not the only factor in determining the electrochemical performance. In association with our XPS analysis of the graphenes shown in Table S1 and Fig. S3 (ESI<sup>†</sup>), with the increase of

pyrolysis temperature from 500 to 900 °C,  $\text{I}_5^-$  can be transformed into  $\text{I}_3^-$ , albeit with a decrease in overall iodine content from 1.21 to 1.05 wt%. These suggest that  $\text{I}_3^-$  has a higher catalytic activity for ORR than  $\text{I}_5^-$ . It may be due to that  $\text{I}_3^-$  has higher a negative charge density than  $\text{I}_5^-$ , can induce relatively higher positive charge density on the graphene surface, and promote the reaction to reduce oxygen to  $\text{OH}^-$ . Moreover, with the sequential increase of annealing temperature from 900 to 1100 °C, we find that the content of proportion of  $\text{I}_3^-$  remains little changed, while the overall iodine content clearly decreases. This may be a prime cause for the lower activity of I-graphene-1100 compared to that of I-graphene-900.

In summary, we have reported a new kind of metal-free I-graphene catalyst, fabricated through a simple, economical, and scalable approach, which boasts a greater ORR electrocatalytic activity than that of current commercial Pt/C catalysts. It also exhibits long-term stability and an excellent resistance to crossover effects for ORRs. Furthermore, our study indicates that the formation of the  $\text{I}_3^-$  structure plays a crucial role for enhancement of the ORR activity of graphene. We believe that iodine-doped carbon materials with a high proportion of  $\text{I}_3^-$  structure prepared through using our or other methods should have even higher electrocatalytic activity for ORR. This new type of heterodoped structure not only enriches the groups involving metal-free ORR catalysts, but also provides more useful information to further clarify the ORR mechanisms of doped carbon materials.

The work was supported in part by grants from NSFC (51002106, 21005055, 21173259) and NSFC for Distinguished Young Scholars (51025207), BSTWZ (G20100191), NSFZJ (R4090137, Y4100520) and ZJED Innovative Team for S. Huang.

## Notes and references

- (a) M. Winter and R. J. Brodd, *Chem. Rev.*, 2004, **104**, 4245; (b) M. Lefevre, E. Proietti, F. Jaouen and J. P. Dodelet, *Science*, 2009, **324**, 71.
- (a) B. Lim, M. J. P. Jiang, E. C. Cho, J. Tao, X. M. Lu, Y. M. Zhu and Y. N. Xia, *Science*, 2009, **324**, 1302; (b) R. Jasinski, *Nature*, 1964, **201**, 1212; (c) J. Lee and T. Aida, *Chem. Commun.*, 2011, **47**, 6757; (d) J. Maruyama and I. Abe, *Chem. Commun.*, 2007, 2879; (e) Y. Y. Liang, Y. G. Li, H. L. Wang, J. G. Zhou, J. Wang, T. Regier and H. J. Dai, *Nat. Mater.*, 2011, **10**, 780.
- (a) K. P. Gong, F. Du, Z. H. Xia, M. Durstock and L. M. Dai, *Science*, 2009, **323**, 760; (b) L. T. Qu, Y. Liu, J. B. Baek and L. M. Dai, *ACS Nano*, 2010, **4**, 1321; (c) R. L. Liu, D. Q. Wu, X. L. Feng and K. Mullen, *Angew. Chem., Int. Ed.*, 2010, **49**, 2565; (d) Y. Q. Sun, C. Li, Y. X. Xu, H. Bai, Z. Y. Yao and G. Q. Shi, *Chem. Commun.*, 2010, **46**, 4740.
- (a) Z. W. Liu, F. Peng, H. J. Wang, H. Yu, W. X. Zheng and J. Yang, *Angew. Chem., Int. Ed.*, 2011, **50**, 3257; (b) L. Yang, S. J. Jiang, Y. Yu, L. Zhu, S. Chen, X. Z. Wang, Q. Wu, J. Ma, Y. W. Ma and Z. Hu, *Angew. Chem., Int. Ed.*, 2011, **50**, 7132.
- (a) C. Lee, X. Wei, J. W. Kysar and J. Hone, *Science*, 2008, **321**, 385; (b) A. J. Patil, J. L. Vickery, T. B. Scott and S. Mann, *Adv. Mater.*, 2009, **21**, 3159; (c) Y. J. Zhang, T. Mori, L. Niu and J. H. Ye, *Energy Environ. Sci.*, 2011, **4**, 4517.
- H. T. Liu, Y. Q. Liu and D. B. Zhu, *J. Mater. Chem.*, 2011, **21**, 3335.
- (a) D. Wang, S. Hasegawa, M. Shimizu and J. Tanaka, *Synth. Met.*, 1992, **46**, 85; (b) X. R. Zeng and T.-M. Ko, *J. Polym. Sci., Part B: Polym. Phys.*, 1997, **35**, 1993.
- (a) N. Jung, N. Kim, S. Jockusch, N. J. Turro, P. Kim and L. Brus, *Nano Lett.*, 2009, **9**, 4133; (b) G. Kalita, K. Wakita, M. Takahashib and M. Umeno, *J. Mater. Chem.*, 2011, **21**, 15209.